DOI: 10.21062/mft.2024.047  http://www.journalmt.com

# Dynamic Analysis of the Propulsion Process of Tunnel Boring Machines

Xiangping Liao (0000-0003-3238-7310)*, Ying Zhao (0009-0000-4409-5038), Shaopeng Kang (0000-0001-5453-1462), Kailei Liu (0000-0002-3503-9891), Xinyang Zhu (0009-0004-5384-4466), Langxin Sun (0009-0008-8784-3110)
School of Mechanical Engineering, Jiangsu University of Technology, Changzhou, 213000, China
*Corresponding Author, Xiangping Liao, Jiangsu University of Technology (School of Mechanical Engineering), Changzhou, 213000, P.R. China, lxp@jsut.edu.cn

**In order to improve the excavation efficiency, and consider the influence of the interference force generated by the propulsion system on the design and service life of key components, it is necessary to correct the trajectory of the tunnel boring machine when excavating curved tunnels. The mechanical model of tunnel boring machine propulsion system is established, and its dynamic characteristics are established by ADAMS software. By analysing the thrust force of hydraulic cylinder (1500KN) and the three steering angles of 0.5°, 1° and 2°, the change of the angle between the thrust hydraulic cylinder and the key components of the gripper shoe hydraulic cylinder is studied, and the relationship between the tightening force and the horizontal propulsion force of the gripper shoe hydraulic cylinder is also studied. The research reveals the difference of the changing laws of propulsive force and tighteningforce under different steering angles. The results are helpful to study the optimal matching relationship between mechanical model and driving parameters of TBM, and have important theoretical significance to further improve the driving efficiency and stability of TBM.**

**Keywords:** TBM, Propulsion process, Thrust mechanism, Propulsion simulation

## 1 Introduction

Full-section tunnel construction technology typically utilizes tunnel boring machines (TBM) to achieve mechanical pressure cutting and rock crushing. Based on large modern loading and transporting machinery as auxiliary equipment, it is a highly mechanized and automatic tunnel excavation equipment, which is complex and has the advantages of high efficiency, speed, safety, and so on [1-2]. Thus, the steps of excavation, slagging, lining, grouting, and so on can be completed at one time [3-4]. However, it is well known that the cost of TBM equipment is very expensive, and the initial investment in TBM construction engineering is even greater. Therefore, the use of motion simulation methods to study the optimal matching relationship between the mechanical model and excavation parameters of TBM during the propulsion process is of great theoretical significance for improving TBM excavation efficiency and stability [5-6]. The dynamic simulation work is completed by ADAMS [7].

Domestic and foreign scholars have conducted a series of studies on TBM gripper-thrust systems. Huang et al [8], established a geometric model for the position in-verse solution of the TBM gripper-thrust mechanism; Wang et al [9], established the motion equations between the thrust cylinder, directional cylinder, and operating parameters of the mechanism. Gao et al [10], established a finite element model of mechanisms under typical configurations using SAMCEF. Farrokh [11] analyzed the actual engineering data of TBM, such as excavation efficiency and speed, and developed a TBM monthly footage prediction model. Zhang et al [12], analyzed the force on a single tool under different surrounding rock conditions and the force on the main machine under a mixed excavation face. In summary, researchers have conducted relevant research on TBM gripper-thrust mechanisms from various aspects, but the simulation model has not been appropriately simplified, resulting in a large workload, and there has been no in-depth research and analysis on the steering conditions of TBM propulsion.

Based on the TBM propulsion system model, a TBM excavation process model was established using ADAMS software, and its dynamic characteristics were analyzed. During the modeling process, the original size was used as much as possible, and some insignificant components were simplified to improve computational speed [13-15]. Under the rated propulsion force and 0.5 °, 1° and 2 ° turning angle, the reasonable matching relationship between the turning angle and the force transfer angle between the hydraulic cylinder and its spherical joint was studied, which could lay a research foundation for further researching the relationship between TBM propulsion force and the tightening force to solve the problem of

TBM gripper Shoe slipping and rock wall collapse. It provides the theoretical value for further improving the tunneling performance of the TBM.

## 2 Establishment of the Propulsion Process Model for TBM

### 2.1 Mechanical Model of Propulsion Mechanism for TBM

The simplified TBM propulsion system is shown in Fig. 1. During operation, the gripper shoes of TBM support both sides of the surrounding rock tightly under the action of the gripper shoe cylinder. Then, under the action of thrust cylinders on the left and right sides of the main beam, the main beam moves forward, and the electric motor drives the cutter head to rotate and cut the rock surface. After advancing one stroke, the rear gripper shoe cylinder that supports the ground extends out. The gripper shoe is retracted and brought back by the gripper shoe cylinders, pushing the thrust cylinder to retract, and the gripper shoe moves forward by one stroke, thus achieving a working circuit process [16].

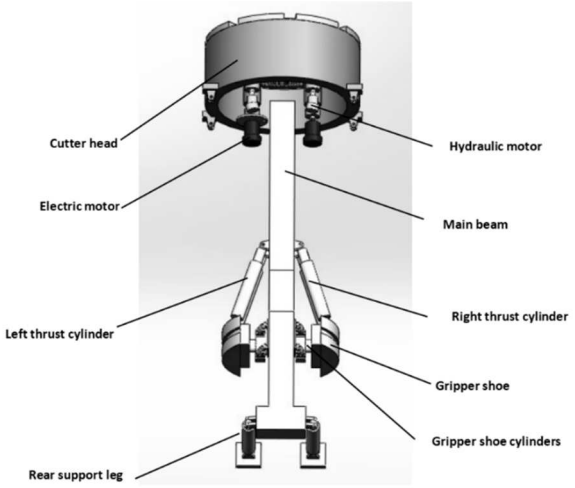


***Fig. 1*** *Diagram of TBM propulsion system*

The external loads that support the propulsion mechanism of TBM during propulsion include the gravity of the mechanism itself, the propulsion and rotational reactions at the cutter head, and the surrounding rock pressure and friction force on the shield, etc. To facilitate mechanical analysis of the propulsion mechanism, the force model of the mechanism can be simplified as follows.

After supporting the surrounding rock tightly with the gripper shoe, the gripper shoe and the surrounding rock are regarded as one entity, which is the fixed end.

Ignoring the gravity of the support and thrust hydraulic cylinder and its spherical joint, the hydraulic cylinder can be considered as a two-force rod.

The pressure and friction force of the surrounding rock surrounding the shield is uniformly distributed around the shield, which can be equivalent to a frictional resistance acting on the center point of the cutterhead.

The force distribution of the simplified TBM support propulsion mechanism is shown in Fig. 2. Establish a spatial coordinate system O-XYZ with the center point O of the cutterhead as the origin, (f0, m0) as the propulsion reaction force and torque of the surrounding rock towards the cutterhead. The point of action of the equivalent friction force between the surrounding rock and the cutterhead shield without considering gravity is O, the unit direction vector is -Y and the size is $F_{f2}$. The point of action of the support force and friction force of the surrounding rock on the shield under the action of gravity is point A, and the unit direction vectors are -Z and -Y, with sizes $F_N$ and $F_{f1}$, respectively. The acting points of gravity on the cutterhead, main beam, and saddle are O, B, and N, respectively, with unit direction vectors of z and sizes of $F_{g1}$, $F_{g2}$, and $F_{g3}$, respectively. The acting point of the propulsion force provided by the gripper shoe to each thrust hydraulic cylinder is $D_i$, the direction unit vector of each propulsion force is $d_i$, the position vector relative to the O point is $l_{di}$, and each propulsion force is $F_{Di}$.The acting points of the force between the hydraulic cylinder and the spherical joint of the shoe support are R and S, and their position vectors relative to the O point are $l_r$ and $l_s$, assuming they have $F_{Rx}$, $F_{Ry}$, $F_{Rz}$, and $F_{Sx}$, $F_{Sy}$, $F_{Sz}$ components in the XYZ direction, respectively. The unit direction vector of the force exerted by the rear supporting system on the propulsion mechanism is y, and the magnitude is $F_{f3}$.

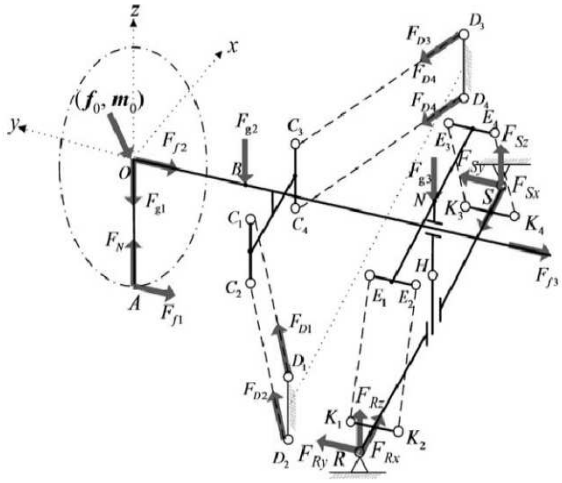


***Fig. 2*** *Schematic diagram of the force acting on the TBM propulsion mechanism*

By balancing the force of the propulsion mechanism in the three directions of x y z, it can be concluded that equation (1). By balancing the torque of the propulsion mechanism at point O, it can be concluded that equation (2).

$$\begin{cases} \sum F_X = 0,\ f_0 \cdot x + \sum_{i=1}^{4} F_{Di} d_i \cdot x + F_{Rx} - F_{sx} = 0 \\ \sum F_y = 0,\ f_0 \cdot y - F_{f1} - F_{f2} + \sum_{i=1}^{4} F_{Di} d_i \cdot y + F_{Ry} + F_{Sy} - F_{f3} = 0 \\ \sum F_Z = 0,\ f_0 \cdot z - F_{g1} + F_N - F_{g2} - F_{g3} + F_{Rz} + F_{Sz} = 0 \end{cases} \tag{1}$$

$$\begin{cases} \sum M_y(O) = 0, \left[ m_0 + \sum_{i=1}^{4} F_{Di}(l_{di} \times d_i) + (F_{Rx} - F_{Sx})(l_r \times x) + F_{Rz}(l_r \times z) + F_{Sz}(l_s \times z) \right] \cdot y = 0 \\ \sum M_Z(O) = 0, \left[ m_0 + \sum_{i=1}^{4} F_{Di}(l_{di} \times d_i) + (F_{Rx} - F_{Sx})(l_r \times x) + F_{Ry}(l_r \times y) + F_{Sy}(l_s \times y) \right] \cdot z = 0 \end{cases} \tag{2}$$

According to equations (1) and (2), the force $F_{Ry}$, $F_{Rz}$, and $F_{Sy}$ between the gripper shoe cylinder and the shoe spherical joint, as well as the relationship between $F_{Sz}$ and the propulsion force $F_{Di}$, can be calculated as follows.

$$\begin{cases} F_{Ry} = \left\{ -\left[ m_0 + \sum_{i=1}^{4} F_{Di}(l_{di} \times d_i) - \left( f_0 \cdot x + \sum_{i=0}^{4} F_{Didi} \cdot x \right)(l_r \times x) + \left( F_1 - \sum_{i=1}^{4} F_{Didi} \cdot y \right)(l_s \times y) \right] \cdot z \right\} / \left\{ \left[ (l_r - l_s) \times y \cdot z \right] \right\} \\ F_{Sy} = \left\{ -\left[ m_0 + \sum_{i=1}^{4} F_{Di}(l_{di} \times d_i) - \left( f_0 \cdot x + \sum_{i=0}^{4} F_{Didi} \cdot x \right)(l_r \times x) + \left( F_1 - \sum_{i=1}^{4} F_{Didi} \cdot y \right)(l_r \times y) \right] \cdot z \right\} / \left\{ \left[ (l_s - l_r) \times y \cdot z \right] \right\} \end{cases} \tag{3}$$

Wherein:

$$\begin{aligned} F_0 &= F_{g1} + F_{g2} + F_{g3} - F_N - f_0 \cdot z \\ F_1 &= F_{f1} + F_{f2} + F_{f3} - f_0 \cdot y \end{aligned} \tag{4}$$

### 2.1.1 Force Simulation Model for the Gripper Shoe of TBM

Taking the gripper shoe as the single body force analysis object, as shown in Fig. 3, it is subjected to the propulsion of the thrust cylinder $F_{D1}d_1$ and $F_{D2}d_2$.

The force acting on the spherical joint of the gripper shoe hydraulic cylinder is $F_{Rx}$, $F_{Ry}$, and $F_{Rz}$. The positive support force of the gripper shoe provided by the side wall surrounding rock is $F_{N1}$; The frictional force of the surrounding rock to the support shoe is $F_{f4}$. The unit direction vector is w, where w is perpendicular to x and the angle between $w$ and z is $\theta w$. Assuming the equivalent maximum static friction coefficient between the sidewall surrounding rock and the gripper shoe is μ.

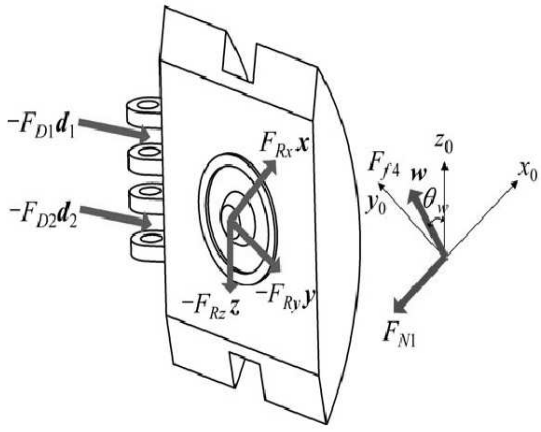


***Fig. 3*** *Schematic diagram of TBM gripper mechanical analysis*

By balancing the three directional forces of the gripper shoe in XYZ, it can be concluded that.

$$\begin{cases} \sum F_x = 0, -\sum_{i=1}^{2} F_{Di} d_i \cdot x + F_{Rx} - F_{N1} = 0 \\ \sum F_y = 0, -\sum_{i=1}^{2} F_{Di} d_i \cdot y - F_{Ry} + F_{f4} w \cdot y = 0 \\ \sum F_z = 0, -F_{Rz} + F_{f4} w \cdot z = 0 \end{cases} \tag{5}$$

The positive support force $F_{N1}$ of the gripper shoe provided by the surrounding rock on the side wall and the friction force $F_{f4}$ of the support shoe need to be met.

The relationship between the tightening force $F_{Rx}$ of the gripper shoe cylinder and the propulsion force $F_{Di}$ of the thrust cylinder can be obtained from equations (5) and (6).

$$\mu F_{N1} \geq F_{f4} \tag{6}$$

$$F_{Rx} \geq \frac{1}{\mu}\sqrt{F_{Rz}^2 + \left(\sum_{i=1}^{2} F_{Di} d_i \cdot y + F_{Ry}\right)^2} + \sum_{i=1}^{2} F_{Di} d_i \cdot x$$
$$\tan\theta_w = \frac{\sum_{i=1}^{2} F_{Di} d_i \cdot y + F_{Ry}}{F_{Rz}} \tag{7}$$

In the process of tunnel excavation, the propulsion force of TBM is transmitted by supporting the surrounding rock with a gripper shoe. Therefore, the stress analysis of the surrounding rock is based on the stress analysis of the gripper shoe. The force of the gripper shoe is mainly composed of three parts: the thrust hydraulic cylinder force $F_3$, the support torque hydraulic cylinder force $F_2$, and the gripper shoe cylinder force$F_1$[17]. The torque hydraulic cylinder is mainly the weight of the supporting main beam and the equivalent force transmitted by the cutter head. Therefore, the force acting on the surrounding rock mainly comes from two parts thrust hydraulic cylinder force $F_3$ and gripper shoe cylinder Force $F_1$ [18].

As shown in Fig. 4, during the tunnel excavation process, the main force of the thrust cylinder on the gripper shoe is $F_3^0$ and $F_3^1$. The angles between them and the direction of the gripper shoe cylinder are α1 and α2, respectively. Under the condition of straight heading and turning, the starting values of α1 and α2 are different, and in the propulsion process $F_3^0$, $F_3^1$ changes with the change of α [19]. On the other hand, in the vertical direction of the surrounding rock, the gripper shoe is mainly supported by the tightening reaction force $F_1^0$and $F_1^1$, and the supporting reaction force is equal in size and opposite in direction under the straight working condition [20]. However, under the condition of horizontal turning, the tightening pressure on the left and right sides will change.

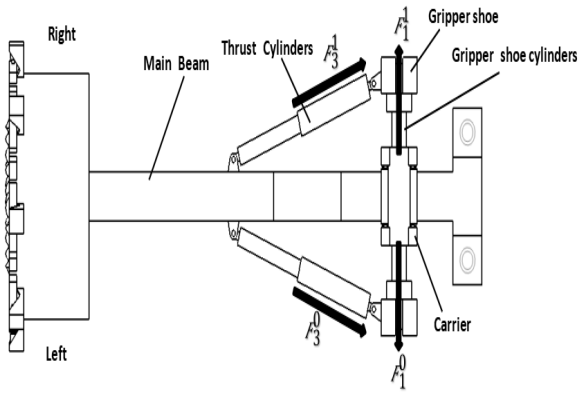


***Fig. 4*** *Schematic diagram of the TBM propulsion system*

## 3 Propulsion Mechanism Model of TBM

For the convenience of analysis, the simulation study was conducted using TBM with a cutter head diameter of 2 meters. The parameters of the relevant data given in the literature combined with the similarity relationship are shown in Tab. 1.

***Tab. 1*** *Simulate TBM technical parameters*

| Force name | Unit | Value |
|---|---|---|
| **TBM Diameter** | m | 2 |
| **Cutter head torque** | KN/m | 160 |
| **propulsion** | KN | 1500 |
| **Promotion step** | mm | 730 |
| **The reaction force of the gripper shoe hydraulic cylinder** | KN | $F_1$=3000 |
| **The reaction force of Torque Hydraulic Cylinder** | KN | $F_2 \in$ [30~60] |
| **Single-thrust hydraulic Cylinder Reaction** | KN | $F_3 \cos a \in$ [600~1000] |
| **The range of angle changes from beginning to end** | ° | α ∈ [15°~25°] |

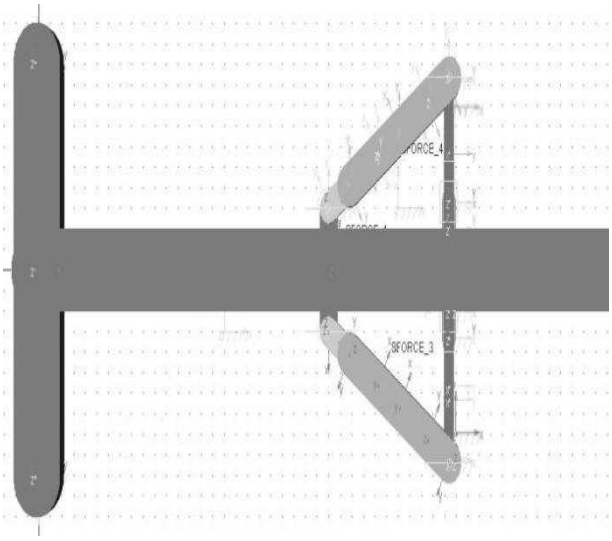

***Fig. 5*** *Schematic diagram of ADAMS simulation model for TBM propulsion mechanism*

In the process of tunnel excavation, there is usually a method of advanced detection to predict the geological situation in the direction of progress, but it cannot avoid unpredictable situations. During tunnel excavation, the disturbance of surrounding soil becomes more severe due to the change of rock mass stress, which causes the tunnel boring machine to deviate from the designed trajectory during the excavation process, affecting the excavation speed and reducing its work efficiency [21-22]. To meet the needs of the actual route forward, it is necessary to correct the deviation from the trajectory [23-24]. Due to the swing of the main beam, the angle between the left and right thrust hydraulic cylinder and the gripper shoe cylinder changes, and the cutter head will produce interference force. To find the relationship between the propulsion force provided by the thrust hydraulic cylinder and the variation of the main beam turning angle. Therefore, this work mainly studies the propulsion in a horizontal state. The model is shown in Fig. 5.

## 4 Analysis of TBM Propulsion Simulation Results

### 4.1 Analysis of Simulation Results of Horizontal Condition of TBM Propulsion Mechanism

Under the rated propulsion reaction force, the tunnel boring machine excavates in a horizontal state, and the optimal propulsion force applied between the thrust cylinders is determined through the motion simulation of the mechanism. The simplified model of horizontal propulsion is shown in Fig. 6.

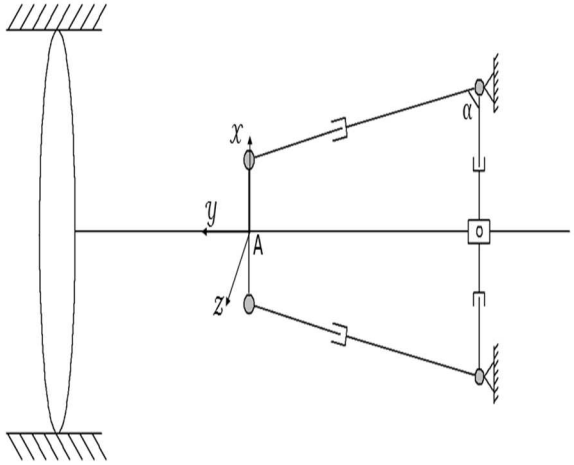


***Fig. 6*** *Simplified model of propulsion in horizontal State*

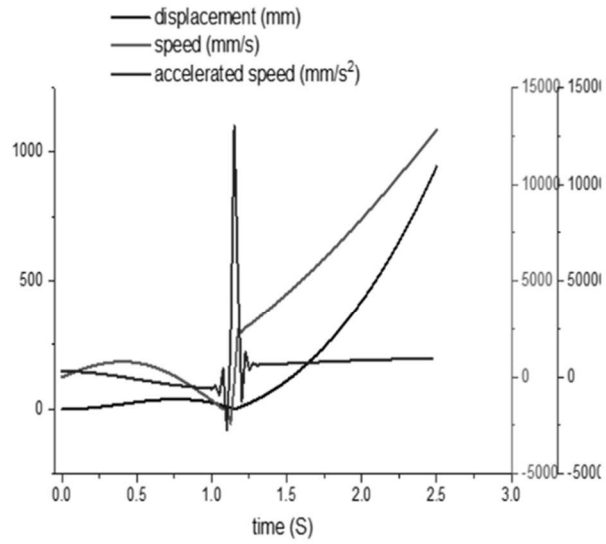


(a) Variation diagram of displacement, velocity, and acceleration changes of the main beam

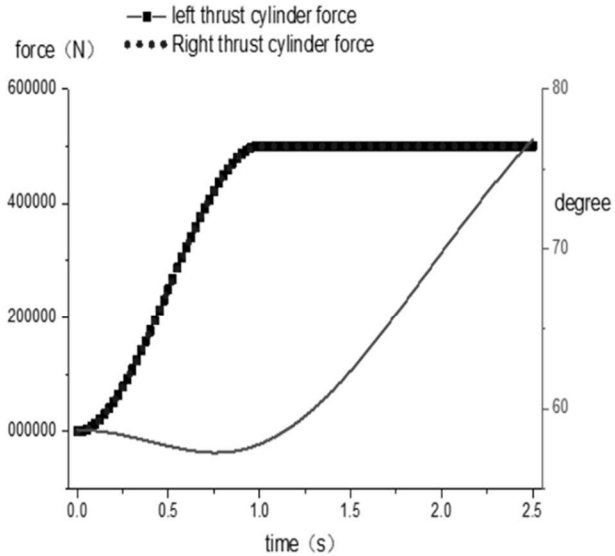


(b) Variation diagram of the angle between the gripper shoe and the thrust cylinder and the propulsion force

***Fig. 7*** *Variation diagram under rated propulsion*

Combining with Fig. 7, we can see that the underrated propulsion reaction, the tunnel boring machine moves in straight line conditions.

When the left and right thrust hydraulic cylinders gradually provide propulsion, the angle first shows a brief narrowing trend. At this point, there is a brief process of overcoming the reaction force of the propulsion force, and then as the propulsion force gradually increases, the reaction force of the propulsion force is overcome. The angle α is steadily changing and increasing, and the entire tunnel boring machine excavation tends to be stable, which is conducive to maintaining the service life of the propulsion mechanism. As can be seen from Fig. 5, when the thrust force is in the range of 1500KN, the displacement of the propulsion is uniform, the speed runs smoothly, and the entire TBM mechanism maintains stable progress during the propulsion process, achieving an ideal propulsion state.

### 4.2 Analysis of Simulation Results after Turning Direction

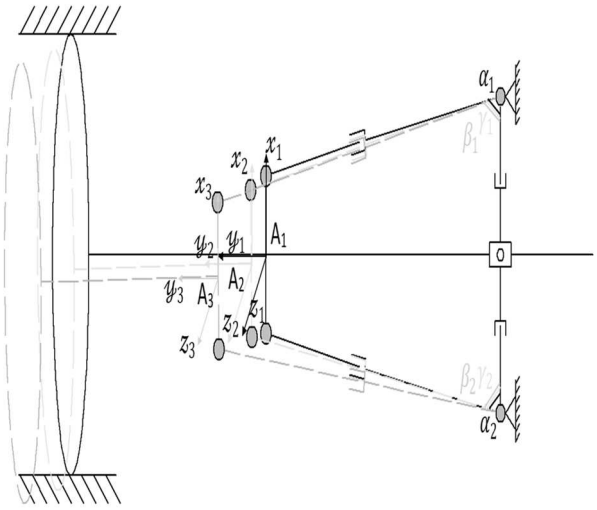


***Fig. 8*** *Simplified model for propulsion under the turning condition*

In the process of tunnel excavation, often when excavating curve trajectory, the trajectory deviation is caused by human operation or natural factors, so it is necessary to correct the trajectory deviation. The trajectory correction mainly realizes this basic function by adjusting the swing of the main beam. Taking point $A_1$ as the center, after adjusting the direction of the main beam, it can be considered that it first rotates to position $A_2$, then advances in a straight line, and then reaches position $A_3$. The schematic diagram of attitude adjustment and propulsion is shown in Fig. 8. In this work, the simulation analysis of the left direction adjustment of the main beam is carried out at 0.5 °, 1 °, and 2 °, and the influence of the main beam direction adjustment on each parameter is studied.

When TBM is in the process of straight heading, the magnitude of the left and right forces of F1 is equal, then turn left adjustment to 0.5 °, 1 °, 2°, as shown in Fig. 9, the force of the left gripper shoe is 465,437 and 391kn respectively, while the force of the right gripper shoe is 528, 565 and 645kn, its force shows a linear trend with the change of angle. Therefore, when the main beam is adjusted to a certain degree, the force acting on the left gripper shoe decreases with the increase of deflection angle, while the force acting on the right gripper shoe increases with the increase of deflection.

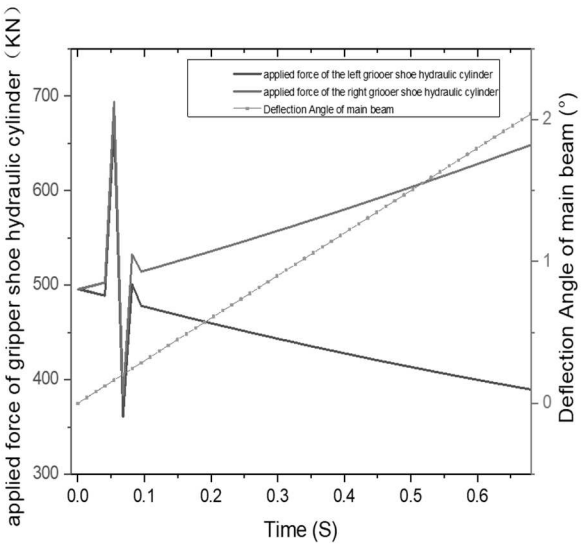


***Fig. 9*** *Diagram of the force acting on the left and right gripper shoes after the main beam turns left*

When the propulsive force provided by the propulsive cylinder is 1500KN, the main beam is adjusted to the left and then pushed back. The angle α between the prop cylinder and the propulsive cylinder has a significant change. When the main beam deflects 0.5 °, 1 °, and 2 °, it can be seen that the angle changes are different in the case of the three curves, The starting angles of $\alpha_2$ were 53.1°,55.9° and 57.2°respectively, while the starting angles of right $\alpha_1$ were 64.7° 61.1°s and 60.1°, respectively, and the angle change of the same curve changes with the change of propulsion displacement. Therefore, as the deflection angle of the main beam increases, the starting left $\alpha_2$ angle increases, while the right $\alpha_1$ angle decreases. But when the main beam advances, its left and right-side angles show an upward trend, as shown in Fig. 10.

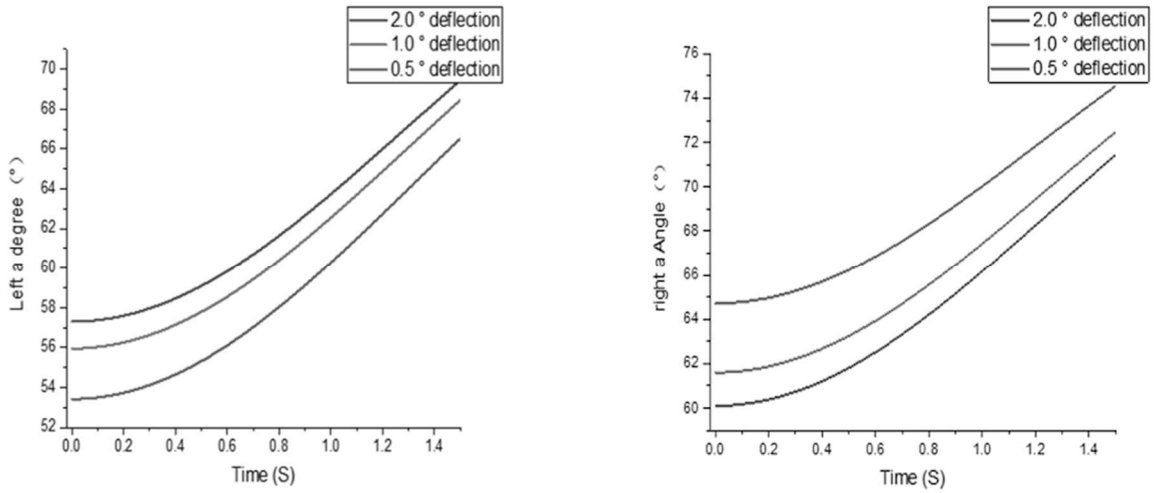


(a) α 2 variation diagram under the deflection of main beam (b) α1 variation diagram under the deflection of main beam

***Fig. 10*** *a variation diagram under the deflection of the main beam*

When the thrust hydraulic cylinder provides a thrust of 1500KN After the main beam deflects 0.5 °, 1 °, and 2 °, The variation of X direction force on three different deflection angle curves with the same displacement of TBM is shown in Fig. 11. It can be seen that the starting force in the Y direction of the left thrust hydraulic cylinder decreases with the increase of the deflection angle, while the starting force in the Y direction of the right thrust hydraulic cylinder increases with the increase of the deflection angle. The starting force in the X direction of the left thrust hydraulic cylinder increases with the increase of the deflection angle, while the starting force in the X direction of the right thrust hydraulic cylinder decreases with the increase of the deflection angle. However, the overall X, Y direction force varies with the change of excavation displacement the magnitude of the X-direction force tends to decrease, and the force in Y direction tends to increase.

It can be seen from the above that when the propulsion force of the mechanism is 1500KN, the propulsion mechanism will run smoothly and the efficiency of the propulsion mechanism will reach the maximum.

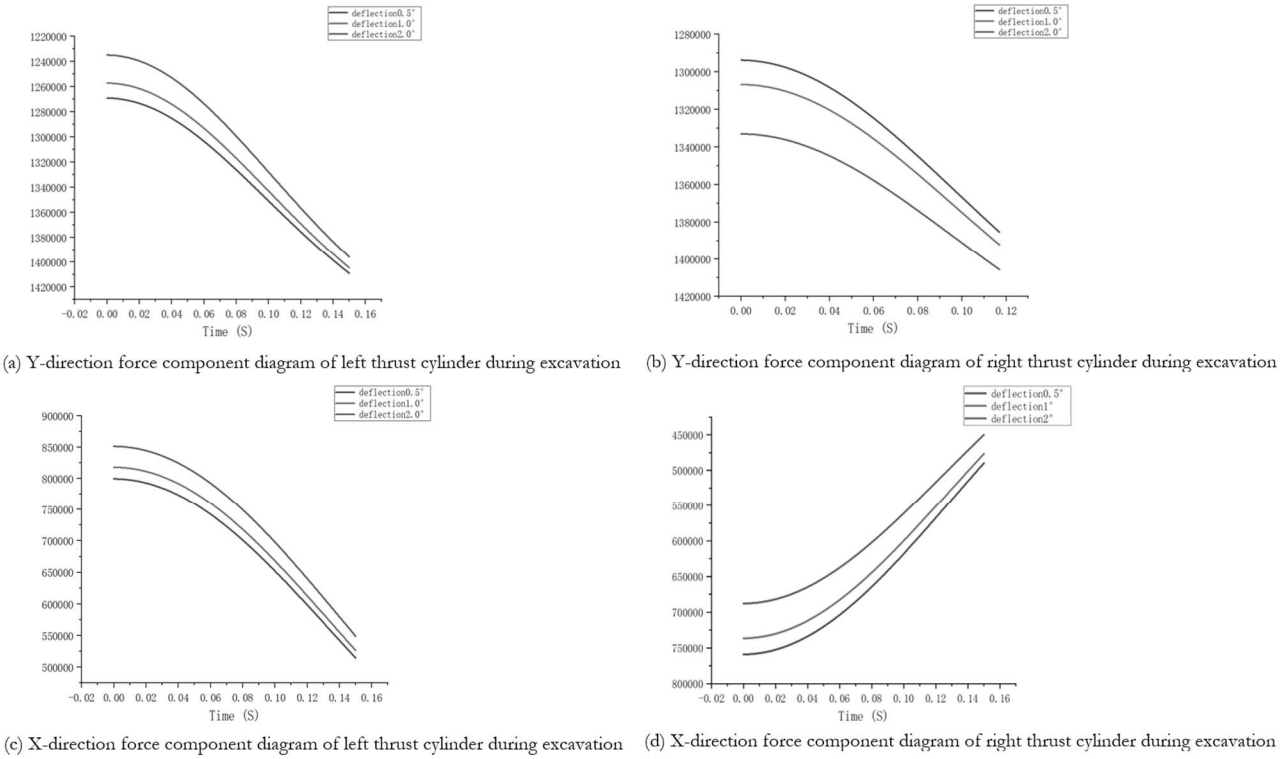


(a) Y-direction force component diagram of left thrust cylinder during excavation (b) Y-direction force component diagram of right thrust cylinder during excavation

(c) X-direction force component diagram of left thrust cylinder during excavation (d) X-direction force component diagram of right thrust cylinder during excavation

***Fig. 11*** *XY-direction force component diagram of left and right thrust cylinder during excavation*

Extracting the propulsion force of each thrust hydraulic cylinder on the gripper shoe from Fig. 9 and 11, the figure shows the numerical value of the maximum thrust force, to make a clearer comparison of the forces exerted on the left and right gripper shoe, draw the stacking diagram of the most powerful thrust hydraulic cylinder in the driving process as shown in Fig. 12. It can be seen that the combined force of the gripper shoe on the surrounding rock fluctuates linearly, when turning the direction to the left by 0.5°,1°,2°, the combined force on the left surrounding rock gradually decreases with the increase of the angle (1264KN>1255KN>1242KN), the right-side increases with the increase of the angle (1821KN<1871KN<1978KN). With the adjustment of the main beam, there is a significant difference in the force exerted by the left and right support shoes on the surrounding rock, so it is necessary to pay attention to the right surrounding rock when the TBM turns left.

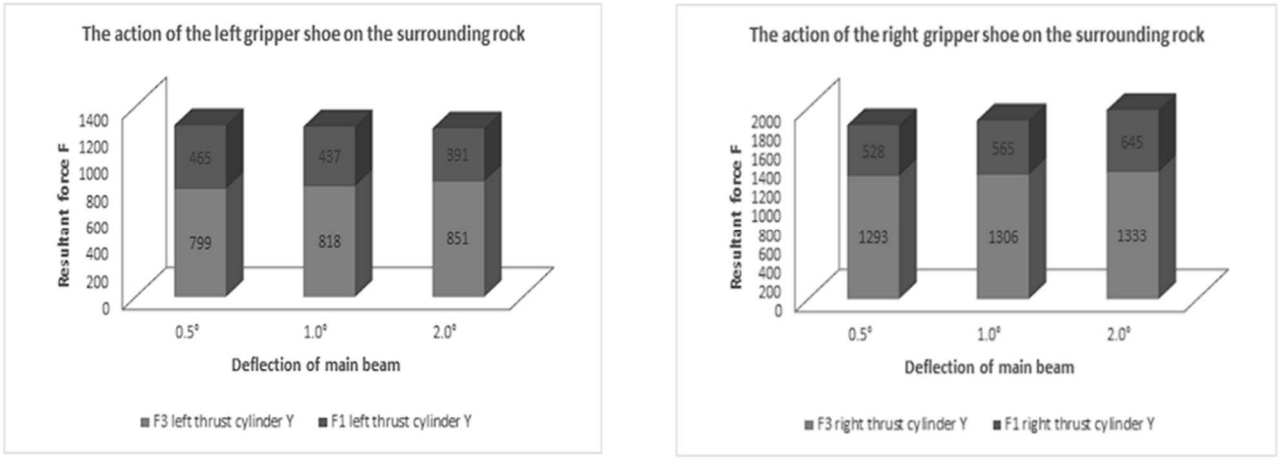


***Fig. 12*** *The force of the gripper shoe on the left and right surrounding rocks*

Although there are advanced testing and exploration techniques to predict the geological conditions of tunneling construction, there are still some unexpected situations. For example, the arch and side walls of the tunnel collapse due to uneven stress, and the disturbance that affects the stratum under harsh underground conditions increases the safety hazards [25-26]. Grasping the relationship between the forces acting on the gripper shoe tunneling system is the key to the successful completion of the established construction tasks.

## 5 Conclusion

In order to study the dynamic propulsion process of TBM, the mechanical model of TBM propulsion system is established in this paper, and the dynamic analysis of TBM excavation propulsion is carried out by ADAMS, and the force relationship between the thrust hydraulic cylinder and the gripper shoe cylinder is deeply simulated and analyzed under the two conditions of straight line and steering.as well as variation law between the corresponding propulsive force and tight force under three different steering angles. The conclusions are as follows.

- Under the rated hydraulic cylinder propulsion force (1500KN), when the TBM is horizontally adjusted to the left at 0.5 °, 1 °, and 2 °, the tightening force of the left gripper shoe F10 (528 KN < 565 KN < 645 KN) decreases with the increase of deflection angle, the tightening force of the right gripper shoe F11 (465KN>437KN>391KN) increases with the increase of deflection angle. The starting left α2 angle increases, while the right α1 angle decreases as the deflection angle of the main beam increases. Both the left and right angle α between the thrust cylinders and gripper shoe cylinders are increasing in the process of tunneling.
- The main beam is adjusted to the left by 0.5°, 1° and 2° respectively under the condition that the gripper shoe hydraulic cylinder remains horizontal and the rated hydraulic cylinder thrust (1500kn). The propulsion force in the X direction of the thrust hydraulic cylinder adjusted to the left direction is larger than that in a straight direction. When the deflection angle increases, the propulsive force F3x in the X direction of the left propulsive hydraulic cylinder increases with the increase of the deflection angle, whereas the propulsive force F3x in the right propulsive hydraulic cylinder decreases with the increase

of the deflection angle. The Y-direction starting force F3y of the left thrust hydraulic cylinder decreases with the increase of the deflection angle, while the Y-direction starting force F3y of the right thrust hydraulic cylinder increases with the increase of the deflection angle.

- Under rated hydraulic cylinder propulsion (1500KN), when the TBM is adjusted to the left by 0.5 °, 1°and 2 °, the difference of resultant force between the left and right gripper shoe is significant. The resultant force of the left gripper shoe decreases with increasing angle (1264 KN, 1255 KN, 1242 KN), while the resultant force of the right gripper shoe increases with increasing angle (1821 KN > 1871 KN > 1978 KN). The force on the left gripper shoe is less than that on the horizontal condition, and the force on the other side is greater than that on the horizontal condition.

Based on the above analysis, future studies can combine the influence of TBM drive system and other factors on the propulsion system, and further optimize the propulsion parameters through actual experimental data. Through the specific propulsion parameters, it is helpful to study the optimal matching relationship between mechanical model and excavation parameters in the process of TBM propulsion, so as to improve the excavation efficiency and stability of TBM, reduce energy consumption and production costs, and improve the economic benefits of industrial production [27].

## Acknowledgement

***This work was supported by the Natural Science Foundation of Hunan Province of China (2021JJ30378), the Research Foundation of Education Bureau of Hunan Province of China (23A0620).***

## References

[1] DU YANLIANG, DU LIJIE. *Full face hard rock tunnel boring machine: system principles and integrated design* [M]. Wuhan: Huazhong University of Science and Technology Press, 2010.

[2] YAO XIAOMING. *Research on TBM construction method in super long tunnel* [D]. Southwest Jiao tong University, 2011.

[3] ZHANG HAOHUANG, LI ZHEN, GAO QINGFENG Application and Development of Full-Face Rock Tunnelling Machine in Domestic Tunnel Engineering [J]. *Mining Machinery*, 2018, 46(7):1-6.

[4] TBM virtual prototype modeling and simulation performance simulation [D]. Zhejiang University, 2016.

[5] LIU Z B, XIE H B, YANG H Y. Simulation analysis of pressure regulation of hydraulic thrust system on a shield tunneling machine [C]// *International Conference* on Intelligent Robotics and Applications. Singapore: Springer, 2009: 493–503.

[6] WANG F, CHEN L Z, WANG K, et al. Rapid finite element modeling method of TBM gripping-thrusting-regripping Mechanism [C]. Proceedings of the 2018 *IEEE/ASME International Conferenc*e on Advanced Intelligent Mechatronics, New York: IEEE, 2018: 340-345.

[7] HUANG T, CAO R, WU X. Design of a Biped Climbing Robot: Simulation, Comparison and Implementation. *Manufacturing Technology*. 2023;23(6):976-988.

[8] HUANG T, WANG X L, LIU H T, et al. Force analysis of an open TBM gripping-thrusting regripping mechanism [J]. *Mechanism and Machine Theory*, 2016, 98: 101–113.

[9] WANG K, YANG Y, HUANG T, et al. Topological structure and kinematic characteristic analysis of TBM gripping-thrusting-regripping mechanism [J]. *Journal of Zhejiang University* (Engineering Science), 2015, 49(10):1870-1877.

[10] GAO X X, YANG Y H. Finite element modeling of the gripping-thrusting-regripping mechanism of TBM based on SAMCEF [C]. *Proceedings* of 8th International Conference on Intelligent Robotics & Applications, Cham: Springer, 2015: 481-488.

[11] EBRAHIM FARROKH, JAMAL ROSTAMI, CHRIS LAUGHTON. Study of various models for HRIS ESTIMATION of the penetration rate of hard rock TBMs. *Tunnelling and Underground Space Technology*, 2012, 30: 110~123.

[12] KAIZHI ZHANG, HAIDONG YU, ZHONG PO LIU, et al. Dynamic characteristic analysis of TBM tunneling in mixed-face conditions. *Simulation Modelling Practice and Theory*, 2012, 18: 1019~1031.

[13] YU XULIN, GUO XIAOPENG, WANG XIAOLIANG. Simulation Analysis of the

Main Propeller of the New TBM Propulsion Mechanism Test Bench[J]. *Mechanical Engineering & Automation*, 2016(6):78-79.

[14] ZHANG L M, WU X G, SKIBNIEWSKI M J. Simulation-based analysis of tunnel boring machine performance in tunneling excavation [J]. *Journal of Computing in Civil Engineering*, 2015, 30(4):04015073.

[15] CEDZO M, JOCH R, TIMKO P, HOLUBJÁK J, CZÁNOVÁ T, ŠAJGALÍK M. Topology Optimization of Gripping Jaws of Industrial Robot. *Manufacturing Technology*. 2023;23(1):25-31.

[16] ZHANG ZHEN GONG GUOFANG, WU WEIQIANG, et al. Attitude Adaptive Control of Propulsion System of Hard Rock Tunnel Boring Machine[J]. *Journal of Zhejiang University* (Engineering Science), 2015, 49(10):1870-1877.

[17] LI WEI. Study on the uniformity of stress distribution on the contact surface between TBM gripper and surrounding rock [D].

[18] YU WEI. Analysis of contact between main beam TBM support and surrounding rock [D]. East China Jiao tong University, 2015.

[19] RAO YUNYI, GONG HOUFANG, et al. Study on the Force of Surrounding Rock of Supporting TBM in Different Digging Conditions[J]. *Construction Machinery*, 2015, 46(2):21-27.

[20] MO H H, Chen J S. Study on inner force and dislocation of segments caused by shield machine attitude[J]. *Tunneling and underground space technology*, 2008, 23(3): 281-291.

[21] SRAMOON A, SUGIMOTO M, KAYUKAWA K. Theoretical model of shield behaviour during excavation. II: Application [J]. *Journal of Geotechnical and Environmental Engineering*, 2002, 128(2): 156-165.

[22] CHEN YUXI, GONG GUO FANG SHI ZHUO, etc. Coordinated control of gripper and thrust system for TBM based on construction data[J]. *Journal of Zhejiang University* (Engineering Science), 2019, 52(2):250-257.

[23] SHI HU, YANG HUAYONG, LONG GUOFANG, et al. Present Situation and Prospect of Key Technology and Simulated Test-bed of Shield Tunneling Machine [J]. *Journal of Zhejiang University* (Engineering Edition),2013,47(05):741-749.

[24] WANG L, YANG X, GONG G, et al. Pose and trajectory control of shield tunneling machine in complicated stratum [J]. *Automation in Construction*, 2018, 93: 192-199.

[25] WU H, HUO J, MENG Z, et al. Load characteristics study with a multi-coupling dynamic model for TBM supporting system based on a field strain test [J]. *Tunnelling and Underground Space Technology*, 2019, 91(SEP.): 103016.

[26] ERIKA P, FEDERICALUCIA S, JIAN Z. Analysis and estimation of gripper TBM performances in highly fractured and faulted rocks [J]. *Tunnelling and Underground Space Technology*, 2016, 52:44–6.

[27] DU Y, LU Z, CHANG E, LI Q, SHI Y. Identification Method of Vibration Drilling Bit Wear State Based on Signal Im-aging and Deep Learning. *Manufacturing Technology*. 2023;23(4):392-398.